Electronic Supplementary Material (ESI) for Soft Matter.
This journal is © The Royal Society of Chemistry 2018

Supporting Information

Yanjun Yang, Herbert Levine

Forces in our model

In our model, every cell is represented by two particles, the front and the rear particle. The polarity of the cell is defined by $\boldsymbol{r} = \boldsymbol{r}_f - \boldsymbol{r}_r$, where $\boldsymbol{r}_f$ and $\boldsymbol{r}_r$ are the positions for the front and rear particles respectively. There is a self-propulsion force $\boldsymbol{m}$ for each particle, m_f for the front particle, m_r for the rear particle. For an isolated cell, the direction for the propulsion force is along $\boldsymbol{r}$ but pointing to opposite directions for the front and rear particles; both particles point away from each other. For cells in a cluster, both the direction and magnitude of the self-propulsion force are regulated by contact inhibition of locomotion CIL (see later). The self-propulsion force is balanced by the intracellular contraction force $\boldsymbol{f}_{contr} = (-f^0_{contr} r/(R_{contr} - r) + f_{exp}/r)\hat{\boldsymbol{r}}$ ($\hat{\boldsymbol{r}} = \boldsymbol{r}/|r|$, is a normalized vector. We use f^0_{contr} for regular cells and f^b_{contr} for boundary cells). This force is attractive for most distance r and only repulsive at extremely short distances, where the repulsion force simulates a hard core.

We distinguish motile and non-motile cells. For a motile cell, we have $m_f > m_r$, while for a non-motile cell, we set $m_f = m_r$. Both m_f and m_r are fixed parameters in our model. Cells can switch between motile and non-motile states. A non-motile cell can transition to a motile cell at a constant probability k_+, and the choice of front and rear particle is set randomly at an equal probability. A motile cell can also become a non-motile cell at a probability depending on the alignment between cell polarity ($\boldsymbol{r}$) and its time-averaged velocity ($\boldsymbol{v_m}$), $k_- = k^0_- exp(-c_{trans}\hat{\boldsymbol{v}}_m \cdot \hat{\boldsymbol{r}})$, where both $\boldsymbol{r}$ and $\boldsymbol{v}_m$ were normalized, i.e. $\hat{\boldsymbol{r}} = \boldsymbol{r}/|r|$ and $\hat{\boldsymbol{v}}_m = \boldsymbol{v}_m/|v_m|$.

The intercellular force between particles from different cells is $\boldsymbol{f}_{adh/rep}(\boldsymbol{r}) = (-A(B-r) + C(B-r)^3)\hat{\boldsymbol{r}}$ for distances within R_{cc} and zero further away. For distance between R_{rep} and R_{cc}, the force is attractive which simulates the cell-cell adhesion. For distance below R_{rep}, the force is repulsive which models the volume exclusion of cells. To account for cells of different lengths, we adjust the units using the length of the longer cell l. We assume $R_{cc} = 1.3l$ and $R_{rep} = 0.75R_{cc} = 0.975l$. We also assume a fixed maximum adhesion value f^{max}_{adh} (the absolute values of the minimum of $f_{adh/rep}(r)$, different values were used for interaction between different kind of cells). Then we have, $B = R_{cc}$, $A = f^{max}_{adh} 3^{3/2}/(2(R_{cc} - R_{rep}))$, and $C = A/(R_{cc} - R_{rep})^2$. For cells shorter than a minimum value $l_{min} = R^{min}_{cc}/1.3$, we

assume $R_{cc} = R_{cc}^{min}$. For cells longer than a maximum value $l_{max} = R_{cc}^{max}/1.3$, we assume $R_{cc} = R_{cc}^{max}$.

The friction between cell and substrate is $\boldsymbol{f}_{fric} = \xi \boldsymbol{v}$, where ξ is a constant for each particle. We assume the friction balances the propulsion force and traction force. Therefore, we can determine the traction force $\xi \boldsymbol{v} - \boldsymbol{m}$ in our model.

The contact inhibition of locomotion (CIL) regulates the self-propulsion force. To calculate the self-propulsion force for each particle i, we first calculate the sum of normalized vector connecting this particle i and its neighboring particles j's (including its partner particle in the same cell) within a distance R_{inh}, i.e. $\boldsymbol{R}_i = \sum_{j, r_{ij} < R_{inh}} \hat{\boldsymbol{r}}_{ij}$. Then the self-propulsion force for particle i becomes $\boldsymbol{m}_i = -m_i \boldsymbol{R}_i / n_i$, where m_i is m_f or m_r depending on whether this particle is a front or rear particle, and n_i is the number of its neighboring particles. We assume $R_{inh} = R_{cc}$ in our model. We can change the level of CIL by varying the weight of the partner particle k within same cell of particle i when calculating $\boldsymbol{R}_i$, i.e. we can have $\boldsymbol{R}_i = c_{inh} \hat{\boldsymbol{r}}_{ik} + \sum_{j \neq k, r_{ij} < R_{inh}} \hat{\boldsymbol{r}}_{ij}$ and $\boldsymbol{m}_i = -m_i \boldsymbol{R}_i / (n_i - 1 + c_{inh})$, where we assign a different weight c_{inh} other than 1 to the partner particle k of particle i. If we set c_{inh} larger than 1, we count the partner particle k with a larger weights, which results in a lower level of CIL. For simulations without CIL, we only count the contribution from the partner particle k when calculating $\boldsymbol{R}_i$, which is equivalent to setting $c_{inh} \gg 1$.

'Boundary cells' and the supracellular actomyosin cable

For circular wounds, we sort particles based on their distance to the wound center, then we define the average distance to the wound center of the first four particles as the wound radius R_{wound}. If a particle has a distance to the wound center below $R_{wound} + d$, we designate the whole cell containing this particle as a 'boundary cell'. If a particle in a 'boundary cell' has a distance to the wound center larger than $R_{wound} + d + \delta$, the whole cell will transit back to a regular cell. Here, d can be considered as the width of the actomyosin cable region, and δ is a parameter we introduce to make the model stable. (i.e. to prevent a cell on the decision boundary from switching back and forth, biologically it corresponds to the delay in this converting.) (Figure S1a) For wounds of other geometries, we define 'boundary cells' in a different way. For each particle, we count the number of other particles within a range of R_{nei}. In Cartesian coordinates, we divide this range into four subregions northeast (NE), southeast (SE), southwest (SW), northwest(NW) and count the total of particles in each subregion (Figure S1b). If the total particles in one subregion is less than the average number of total particles in other three subregions by 5 or the total particles in two adjacent subregions is less than the total particles in the other two adjacent subregions by 8, we designate the cell

containing this particle as a 'boundary cell'. If a particle from a 'boundary cell' picks up a balanced number of surrounding cells in all four subregions, i.e. the difference between the total particle number in any subregion and the average number of total particles in the other three subregions is less than 2, the cell will transit back to a regular cell. This mechanism is simple to apply and can be used in various geometries, but does not allow us to directly control the width of the actomyosin cable region.

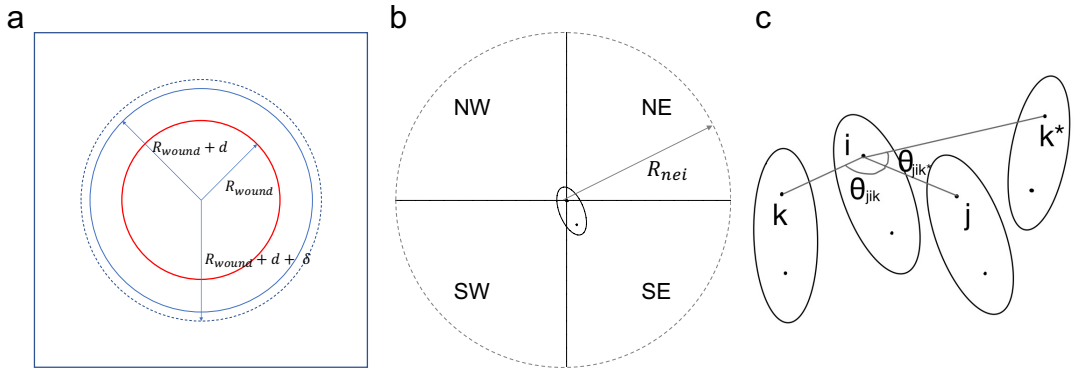

Figure S1: **Cartoon for the wound and 'boundary cells'** **a.** The wound and regions of 'boundary' cells. **b.** Subregions around a particle **c.** Example for deciding unhidden nearest neighbors, where k is an unhidden nearest neighbor of i and k^* is not.

To construct the supracellular actomyosin network, we connect particles from 'boundary cells' with each other's unhidden nearest neighbors. To find out each particle's unhidden nearest neighbors, we first sort all particles (excluding the partner particle) around particle i based on their distance to particle i. Then we find the nearest particles that is not hidden by other nearest particles by applying the following procedure: (1) Calculate the angle θ_{jik} between the line connecting the new particle k and i and the line connecting an already selected particle j and i. (2) If for all j, θ_{jik} is larger than 90°, we select particle k as particle i's unhidden nearest neighbor. (3) Repeat this procedure until we find all the unhidden nearest neighbors (Figure S1c). After finding all the nearest neighbors for each 'boundary cell', we apply an additional intercellular force between these particles, $\boldsymbol{f}_{cable} = (-f^0_{cabcontr} r/((R_{cabcontr} - r)r) + f_{cabexp}/r)\hat{\boldsymbol{r}}$. This additional intercellular force behaves like the intracellular contractive force; it is attractive for most distances and repulsive only for extremely small distances.

The average number of connections between 'boundary cells' reflects the strength of the supracellular actomyosin cable. The number of connection that occur during the wound closing process can be affected by the strength of cell crawling. On the other hand, the strength of this cable will also provide feedback to the effi-

ciency of cell crawling. In addition to such intrinsic interplay between the cable and cell crawling, we can also tune the cable strength in our model. To do this, we change the number of connections between 'boundary cells', for example, we can make it that only front particles can connect with each other, in this way the total connections will drop to about one quarter of the original setting.

We also model the cell-cell adhesion for 'boundary cells' in our simulation. We change the maximum cell-cell adhesion f_{adh}^{max} between two 'boundary cells' and between a 'boundary cell' and a regular cell. We only change the attractive part of the intercellular force; we use the value between two regular cells for the repulsive part. We do this because this repulsion force models the volume exclusion between two cells and it should not depend on cell-cell adhesion.

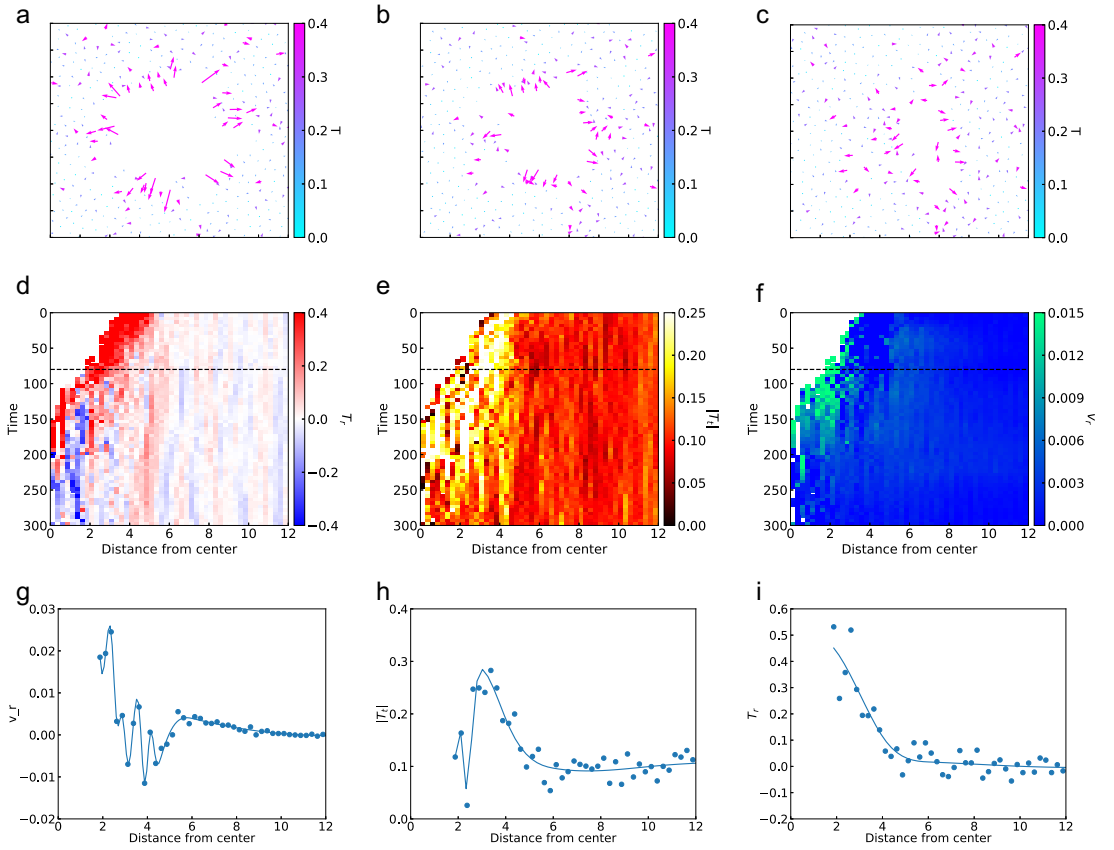

Figure S2: **Traction force for 'boundary cells' with a weaker cell-cell adhesion and intracellular contraction. a-c.** Traction force patterns at three different time points: t=20, t=70 and t=120; color is based on the magnitude, and positive forces point away from the wound center. **d.** Kymograph for the radial component of traction force T_r. **e.** Kymograph for the tangential component of traction force $|T_t|$. **f.** Kymograph for the radial component of the cell velocity v_r. **g.** T_r across the horizontal dashed line in **d**. **h.** $|T_t|$ across the horizontal dashed line in **e**. **i.** v_r across the horizontal dashed line in **f**. The solid lines in **g-i** are merely guides to the data. In this simulation, $f_{adh}^{max(0b)} = 0.7$, $f_{adh}^{max(bb)} = 0.7$, $f_{contr}^{b} = 1.0$, and other parameters are same as in Table S1.

Table S1: Simulation parameters in simulation units used in Figure 2.

Parameter	Value	Unit	Meaning
m_f	1.5	$p_0 l_0$	Magnitude of propulsion force of front particle for motile cells
m_f	1.3	$p_0 l_0$	Magnitude of propulsion force of front particle for non-motile cells
m_r	1.3	$p_0 l_0$	Magnitude of propulsion force of rear particle
f_{exp}	0.02	$p_0 l_0^3$	Cellular expansion coefficient
f_{contr}^0	1.0	$p_0 l_0^2$	Cellular contraction coefficient for regular cells
f_{contr}^b	2.5	$p_0 l_0^2$	Cellular contraction coefficient for boundary cells
R_{contr}	2.5	l_0	Maximum distance for intracellular contraction
k_+	0.1	$1/t_0$	Transition rate to motile state
k_-^0	0.1	$1/t_0$	Transition rate to nonmotile state for zero velocity
c_{trans}	5.0		Scaling parameter for transition to nonmotile state
$f_{adh}^{max(00)}$	0.7		Maximum cell-cell adhesion between two regular cells
$f_{adh}^{max(0b)}$	4.2		Maximum cell-cell adhesion between a regular cell and a boundary cell
$f_{adh}^{max(bb)}$	5.6		Maximum cell-cell adhesion between two boundary cells
$f_{cabcontr}^0$	5.0	$p_0 l_0$	Cable contraction coefficient for the supracellular cable
f_{cabexp}	0.12	$p_0 l_0^3$	Cable expansion coefficient
$R_{cabcontr}$	3.5	l_0	Maximum distance for supracellular cable contraction
R_{cc}^{min}	0.7	l_0	Minimum interaction range for small cells
R_{cc}^{max}	1.1	l_0	Maximum interaction range for large cells
R_{cc}	$1.3l$	l_0	Range of adhesive intercellular force
R_{rep}	$0.75R_{cc}$	l_0	Range of repulsive intercellular force
R_{div}	0.9	l_0	Threshold distance for cell division
k_{div}	0.002	$1/t_0$	Division rate for cells surpassing size threshold
R_{inh}	$1.3l$	l_0	Contact inhibition range
ξ	3.0	$p_0 l_0 t_0$	Friction coefficient with the substrate
t_{relax}	50.0	t_0	Relaxation time for velocity averaging
R_{wound}	5.0	l_0	Radius of the circular wound
$R_{non-adh}$	0	l_0	Radius of the non-adhesive region
d	1.0	l_0	Width of the boundary cell region
δ	0.5	l_0	Buffer zone width of the boundary cell region
R_{nei}	2.0	l_0	Boundary cell neighbor range
c_{inh}	1.0		Level of CIL (CIL becomes lower as c_{inh} gets larger)